

Deep inelastic neutron scattering on liquid hydrogen in the crossover region between the molecular and atomic regimes

U. Bafile, M. Celli, and M. Zoppi

Consiglio Nazionale delle Ricerche, Istituto di Elettronica Quantistica, Via Panciatichi 56/30, I-50127 Firenze, Italy

J. Mayers

Rutherford Appleton Laboratory, ISIS Neutron Facility, Chilton, Didcot, OX11 0QX, United Kingdom

(Received 4 September 1997)

We have measured the double differential cross section of liquid hydrogen using deep inelastic neutron scattering in an intermediate region of momentum and energy transfer where the crossover between the molecular and atomic regimes is expected. The range of the momentum transfer, computed on the basis of the atomic recoil, is between 24.6 and 36.2 \AA^{-1} , i.e., beyond the limit where intermolecular interactions are effective and therefore the incoherent scattering approximation applies. The data cannot be reproduced either using a molecular or an atomic model. We find that a satisfactory fit to the data is obtained by a linear combination of the two models. The relative weight of the molecular model turns out a decreasing function of the energy transfer. [S0163-1829(98)03226-3]

I. INTRODUCTION

Deep inelastic neutron scattering (DINS) is an experimental technique where the momentum and the energy transferred from the neutron to the target nucleus is so large that all the *intermolecular* and *intramolecular* interactions are considered negligible.¹⁻³ In fact, the intermolecular interactions are known to affect the neutron scattering cross section in a rather restricted range of momentum transfer $\hbar q$ where the intermolecular structure factor $S(q)$ is sensibly different from 1.

If the system is monatomic $S(q)$ extends typically up to 10–15 \AA^{-1} . Beyond this point, the system behaves as an ensemble of independent particles and the incoherent approximation applies. A further increase of the momentum transfer moves the system within the applicability limit of the impulse approximation (IA). In truth, this approximation holds only in the limit $q \rightarrow \infty$ and, for finite values of q , final state effects (FSE) should be taken into account.³ Within the IA, the scattering cross section becomes that of a recoiling particle, with a peak centered at the recoil energy $\hbar\omega = (\hbar q)^2/2m$ and a shape that is determined by the momentum distribution of the particles, m being the mass of the atoms. DINS can be used to measure the momentum distribution of those monatomic systems (quantum solids and fluids) that are known to deviate from the classical Maxwell-Boltzmann distribution.⁴ This technique has been extensively used to determine the momentum distribution of solid,⁵ liquid,⁶ and gaseous^{7,8} helium at low temperature.

In a molecular system, because of the intramolecular interactions, the range of the coherent scattering extends to a larger q range (see for example, Ref. 9). Therefore, the applicability range of the IA is pushed towards higher q values. However, neutron scattering experiments can be carried out, using large momentum and energy transfer, so that the applicability limit of the IA can be reached. Recent DINS experiments on molecular hydrogen have been performed with

the aim of obtaining information on the momentum distribution of the molecular center of mass.¹⁰ In this regime the IA can be still applied and the width of the scattering function is determined by a complex balance between the *translational* and *rotovibrational* terms determining the momentum distribution of the struck molecule. Using this technique, the density evolution of the molecular kinetic energy of liquid hydrogen has been obtained experimentally.¹¹

Using the modern neutron spallation sources, the momentum transfer can become so high that even the intramolecular structure becomes negligible. In this case, the spectrum becomes again that of a recoiling particle, with a characteristic peak centered at the energy $\hbar\omega = (\hbar q)^2/2m$, m being the mass of the target nucleus.¹²⁻¹⁵ This relation has been verified both on hydrogen¹⁴ and deuterium.¹³ In this case, since the intramolecular kinetic energy terms are much larger than the corresponding translational counterparts, the information concerning the momentum distribution of the molecular center of mass is hidden.¹⁴

It is worthwhile to compare the analysis of the various experiments for different values of q . In the relatively low q range, where the molecular momentum distribution becomes accessible, the data are interpreted using the IA together with a molecular model where the intramolecular excitations are uncoupled from the translational dynamics. Within this model, the positions of the various molecular transitions are observed to evolve, in a E vs q^2 plot, following a straight line with a slope corresponding to the *molecular* mass (see Fig. 2 of Ref. 10). Conversely, in the much higher q region of the experiments carried out using spallation-source neutrons, the recoil peak position is observed, in a similar plot, to evolve following again a straight line but now with a slope corresponding to the *atomic* mass (see Fig. 1 of Ref. 14 and Fig. 3 of Ref. 13).

In one case, a suitable molecular model is expected to describe the scattering cross section. This happens when the momentum transfer is so low that the molecule reacts as a

whole to the scattering event. In the other case, an atomic model would be more appropriate. In other words, it may happen that the momentum transferred by the neutron is so large that either the molecule breaks into its components or the scattering event is so fast that the final state of the struck nucleus is better described by a free particle model. One would expect that there exists an intermediate q range where the behavior of the molecular hydrogen cross section changes from the molecular to the atomic regime. In order to study this very interesting crossover between the two regimes, we have started an experimental investigation of DINS on hydrogen in a range of relatively low momentum transfer. Here, we report the results of this experiment, in an effort to study the inelastic neutron cross section of molecular hydrogen in that region of q that is intermediate between the molecular and the atomic regimes.

II. DESCRIPTION OF THE EXPERIMENT

The experiment was carried out on the inelastic resonance spectrometer eVS at the spallation neutron source ISIS. This is an inverse geometry spectrometer whose useful incident beam energy ranges between 1 and 100 eV.¹⁶ A thin uranium foil, on the secondary beam, is used as a resonance absorption filter and is moved cyclically in and out with a periodicity of 10 min. The lowest energy resonance of the uranium foil is rather high ($E=6.671$ eV) and therefore, in order to decrease the range of the momentum transfer, we used a special instrument configuration, placing the detectors at the lowest possible scattering angles. This is in the interval $\theta \approx 23^\circ - 32^\circ$. An alternative configuration of the instrument, namely, using a gold foil as energy analyzer, would have been more suitable to decrease the momentum transfer ($E=4.922$ eV). However, the width of the absorption line of gold is much broader than that of uranium and we would have lost in the instrumental resolution.

It is well known that lowering the scattering angle corresponds to a degradation of the instrument resolution. In order to compensate for this effect, we also designed a further nonstandard working configuration on the geometry of the instrument. To this aim, the detector banks were moved as far as possible from the sample ($L_1 \approx 120$ cm). As a result, the angular contribution to the instrument resolution function turned out always smaller than (though similar to) the intrinsic energy term. Finally, it turned out that the contribution to the resolution function from the primary path (L_0), the secondary path (L_1), and the time of flight (τ) were 3 to 5 times smaller than both the angular contribution (determined by the combined size of the sample and the detectors) and the intrinsic energy contribution (determined by the absorption linewidth of the uranium foil). The total resolution figure was evaluated by assuming a convolution of five Gaussian functions,¹⁷ using a Monte Carlo simulation routine. In Table I, we report the experimental configuration of the present experiment, together with the computed width (standard deviation) of the resolution function. This quantity is named σ and was evaluated computing the function $d^2\sigma/d\Omega dE$ for a sample with a momentum distribution represented by a δ function.

The sample (liquid hydrogen) was held in an aluminum cylindrical container (external diameter 8 mm, internal diam-

TABLE I. Parameters describing the present experimental configuration on eVS. The primary path is $L_0=11.055$ m. The time offset has been assumed constant and equal to the average of the measured values $\tau_0 = -4.7$ μ s. The instrument resolution is given by σ . This is the standard deviation of the calculated Gaussian that was evaluated computing the function $d^2\sigma/d\Omega dE$ for a sample with a momentum distribution represented by a δ function. The energy contribution (absorption width of the uranium foil) is $\sigma_E = 63.0$ meV. In the last two columns we report, for completeness, the values of the momentum and energy transfer computed for the recoil of atomic hydrogen.

Spectrum	θ (deg)	L_1 (m)	σ (meV)	q_{peak} (\AA^{-1})	ΔE_{peak} (eV)
9	23.41	1.242	100	24.57	1.251
8	24.26	1.230	102	25.57	1.356
10	24.45	1.243	103	25.80	1.380
7	25.48	1.230	106	27.04	1.516
11	25.65	1.245	106	27.25	1.539
6	26.68	1.231	108	28.51	1.686
12	26.78	1.246	109	28.64	1.701
5	27.84	1.231	112	29.97	1.862
13	27.89	1.248	112	30.03	1.870
4	29.02	1.231	117	31.48	2.055
14	29.03	1.249	117	31.49	2.057
15	30.18	1.251	121	33.00	2.258
3	30.20	1.231	121	33.03	2.262
16	31.34	1.252	125	34.56	2.476
2	31.36	1.231	126	34.58	2.480
1	32.53	1.232	130	36.19	2.716

eter 6 mm) fitted into a liquid helium cryostat. The scattering cell was connected to the external gas handling system by means of a 1/8 in. OD stainless steel tube. The filling tube was wrapped with an electric heater in order to avoid blockage. The upper body of the cell, connected to the center stick of the cryostat, was temperature controlled and stabilized at 20.0 K. Inside the scattering cell, out of the neutron path, we inserted a solid catalyst ($\text{Cr}_2\text{O}_3 \cdot \gamma\text{Al}_2\text{O}_3$) in order to increase the rate of conversion from *ortho*- to *para*-hydrogen.

The advantage of working with almost pure *para*-hydrogen is that only one rotational state ($J=0$) is populated. In this case, the theoretical calculations become simpler and the comparison between theory and experiments is much more clean. The thermodynamic equilibrium composition of hydrogen, near to the triple point, is very close to 100% concentration of the even- J *para* species. However, the natural rate of conversion between odd- and even- J states of hydrogen is very slow and it may take many days.¹⁸ Using a catalyst makes the rate of conversion faster and helps in producing an equilibrium mixture in a more reasonable time.

Liquid hydrogen was condensed directly into the scattering cell by cooling the sample under a moderate constant pressure of gas. The liquid sample was then subjected to small rapid temperature variations so that the induced turbulence led to a continuous and efficient interaction with the catalyst. Basing on a previous experience we were confident that the equilibrium *ortho-para* composition was obtained in a few hours.¹⁹ The pressure of the sample was then set at $p=3.6$ bar, slightly above the value of the saturated vapor pressure at 20 K ($p_{\text{sat}}=0.935$ bar) to ensure that the scatter-

ing cell was filled with liquid. The corresponding molecular number density is²⁰ $n = 21.23 \text{ nm}^{-3}$.

The data acquisition was carried out in subruns of the order of 12 h ($\sim 2000 \mu\text{A h}$ of integrated proton current). The total acquisition time (sample) was of 137 h, corresponding to a total integrated proton current of 25.259 mA h. The temperature stability during the whole experiment was found to be better than 0.1 K. However, we observed small fluctuations in the pressure reading. This was attributed both to changes in the flux of liquid helium through the throttle valve of the cryostat, and to small changes in the room temperature of the experimental hall. At any rate, a thorough analysis of the different subruns did not show any appreciable effect in the spectra and the differences were always below the statistical noise. This is also due to the fact that a change of 0.1 bar would produce a change in density of the order of 0.02%.

The instrument calibration is carried out using the four lowest energy absorption lines of a thin uranium foil placed in the incident beam. This is usually done using a thin slab sample made of lead, for which one assumes elastic scattering, corrected for the effect of the recoil using the IA. In this way, the geometrical parameters of the instrument can be derived. Since the primary path L_0 is known, this reduces to the determination of the secondary path L_1 and the time offset τ_0 . The angular position of the detectors is also obtained measuring the position of the Bragg peaks of the same Pb sample. In our case, however, we found that this calibration procedure brought evidence of a slight systematic error in the scattering angles. This was found by comparing the data of the right and left detector banks. We attributed this discrepancy to the extended size and the different geometry with respect to the hydrogen sample of the Pb target that was used for the calibration. For this reason, we carried out a second calibration procedure using the sample container, made of aluminum alloy, as a standard. As a result, most of the observed systematic discrepancy between the two detector banks were removed, even if the geometrical parameters of this second calibration were found not much different from the previous ones. For the sake of completeness, we report in Table I the results of the calibration. In the last two columns, we report the theoretical values of the momentum (in \hbar units) and the energy transfer at the position of the recoil peak for atomic hydrogen. We observe that the q interval ranges between ~ 25 and $\sim 36 \text{ \AA}^{-1}$, i.e., well below the expected limit of validity of the IA for the atomic regime. Correspondingly, the energy transfer on the atomic recoil peak ranges between 1.2 and 2.6 eV, i.e., well below the molecular dissociation threshold of 4.75 eV. As a comparison, the experiment of Ref. 10 was carried out in the q range $5\text{--}17 \text{ \AA}^{-1}$, while the previous eVS experiments on hydrogen were characterized by a much higher q range ($31\text{--}79 \text{ \AA}^{-1}$ in Ref. 13 and $35\text{--}67 \text{ \AA}^{-1}$ in Ref. 14).

III. DATA ANALYSIS

For each detector, the TOF spectra of the different subruns were first visually compared to check for possible differences. No significant instrumental drift was observed and the various spectral data were then added together to reduce the statistical errors. In Fig. 1 we report, as an example, one

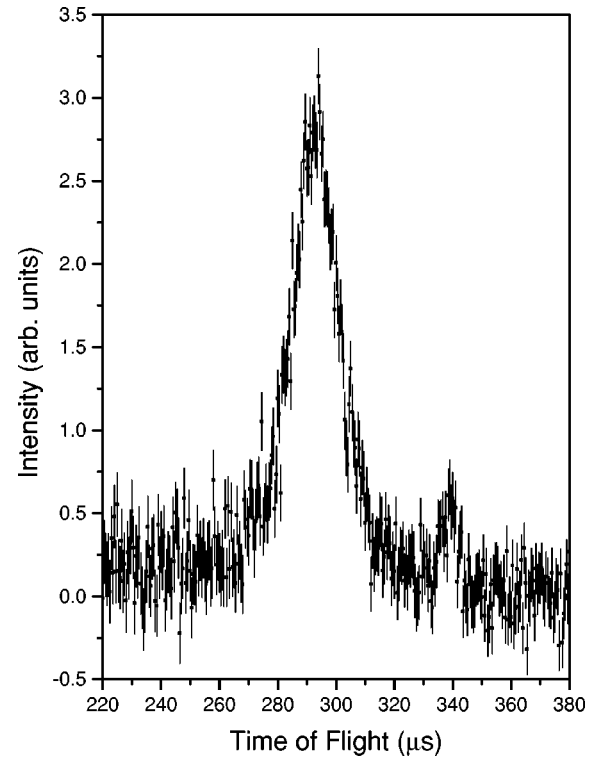


FIG. 1. Time of flight spectrum of liquid *para*-hydrogen in the region of the first resonance absorption of the uranium foil ($E_1 = 6.771 \text{ eV}$). The small structure on the right of the principal peak is the recoil spectrum of the aluminum container. The scattering angle is $\theta = 32.53^\circ$ and the value of the momentum transfer, evaluated on the recoil peak of atomic hydrogen, is $q = 36.19 \text{ \AA}^{-1}$. See Table I.

of the TOF difference spectra (detector No. 1) in the region of the lowest absorption line of the uranium foil. The little structure, on the right of the main peak, is due the container contribution and was easily subtracted. Then we observed the presence of a very small offset in the spectrum baseline that is attributed to multiple scattering. This is not very large and is of the same order of magnitude of the standard deviations of the experimental points. Also this contribution was subtracted. The order of magnitude of the intensity and the shape of the multiple scattering has been confirmed by the results of a Monte Carlo simulation.

The TOF data were first transformed in units of the cross section $d^2\sigma/d\Omega dE$ at constant scattering angle and constant final energy E_1 . The sixteen spectra so obtained were compared with the two available theoretical models. On one side, we computed the measured quantity using a modified version (MYK)²¹ of the Young and Koppel (YK) model.²³ This is a molecular model where the spin correlations, rotations, and vibrations are taken into account exactly, to the extent that vibration-rotation coupling can be neglected and that the vibrations can be considered harmonic.

In the original work by Young and Koppel, a perfect gas model (no intermolecular interactions) was assumed for the translational dynamics. However, it is well known that the contribution from the isotropic potential is the leading term of the intermolecular interactions, as hydrogen, even in the condensed phases, behaves as a free rotor.²⁴ We have generalized the YK model taking into account the isotropic com-

ponent of the intermolecular potential.²¹ In fact, by means of path integral Monte Carlo (PIMC) simulations, we are able to compute the effective kinetic energy of the molecular center of mass of molecular hydrogen.^{25,26} This value can be used to define an effective temperature T_{eff} according to the equation

$$\langle E_k \rangle = \frac{3}{2} k_B T_{\text{eff}}. \quad (1)$$

This effective temperature ($T_{\text{eff}} = 40$ K) is used in the width of the translational Gaussian distribution in place of the true temperature. This simple approximation becomes better and better as the energy and momentum transfer increase and the effect of the interactions on the intermolecular structure decreases. A further improvement of the model was also obtained using, for the vibrational and rotational levels, the measured correction terms that account for the centrifugal distortion and the anharmonicity corrections.²¹

A different model which assumes that the final state of the struck nucleus is described by a plane wave, should be more effective to represent the case where a large momentum is transferred from the neutron to the target nucleus. This model, that was introduced by Andreani, Filabozzi, and Pace (AFP)¹³ to compute the DINS cross section of hydrogen and deuterium in the limits $T=0$ and $q \rightarrow \infty$, was recently generalized to finite temperature and momentum.¹⁵ The model is based on the rationale that, in the IA regime, the scattering event is so fast that the final state of the struck nucleus is described, to a good approximation, by a free-particle wave function. However, even though such a formalism would be able to describe a situation where the molecule is dissociated by the scattering event, in this case it is sufficient to assume that the plane wave description holds in a small region of space close to the initial position of the particle.²²

Both models have been used to compute the inelastic scattering cross section of liquid hydrogen $d^2\sigma/d\Omega dE$ at constant scattering angle and constant final energy E_1 , and at $T=20$ K ($T_{\text{eff}}=40$ K). The scattering angles, used in the computation, were taken from Table I. Since the sample was almost pure *para*-hydrogen (the equilibrium concentration at $T=20$ K is $\approx 99.8\%$ *para*-hydrogen) we assumed in the calculation that only the initial states with $J=0$ and $v=0$ are populated. The computed spectra were then convoluted with the instrument resolution function and these results were compared with the experimental spectra.

In Fig. 2 we show this comparison for spectrum No. 2. The dots with the error bars are the experimental cross section data. The line on the left represents the results using the molecular MYK model, while that on the right is obtained from the atomic AFP model. It is important to note that, in both models, *no fitting parameter is used* and that the calculation is based only on the molecular properties of hydrogen and on the numerical value for the translational kinetic energy (i.e., T_{eff}) that was obtained from our PIMC simulation. We observe that neither model is able to give a satisfactory description of the experimental spectrum. Starting from the low-energy side, the experimental points follow the molecular model up to about one half of the peak height. However, the experimental spectrum soon becomes lower, broader, and characterized by a peak position at higher energy. Con-

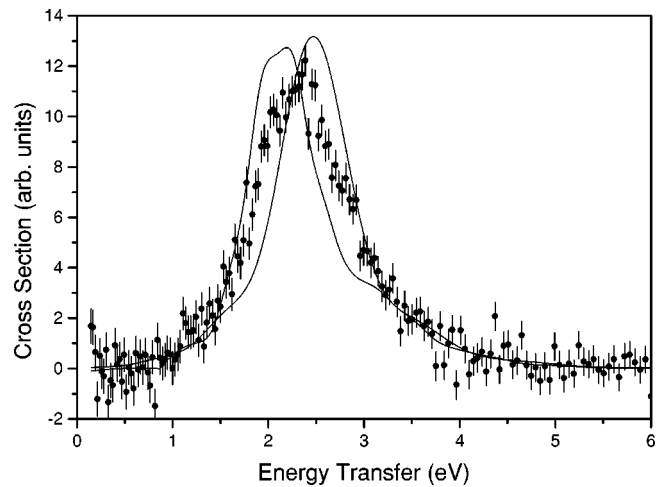


FIG. 2. DINS cross section of liquid hydrogen. The scattering angle is $\theta = 31.36^\circ$. The dots with error bars are the experimental data [normalized using the B factor defined in Eq. (4)]. The line on the left represents the results of the molecular (MYK) model. That on the right is obtained from the atomic (AFP) model.

versely, the peak of the atomic model is found at higher energy than in the experiment. Also in this case, the experimental distribution is wider than the model. However, the final decay of the experimental points follows more closely the atomic model than the molecular one. Similar considerations apply equally well to all the observed spectra. As an example, in Fig. 3 we have reported the spectrum No. 9. Here the scattering angle is smaller and therefore some molecular structure could be visible, as it can be inferred by the appearance, in the experimental spectrum, of a double peak (1.0 and 1.25 eV) and some structure at low energy (0.7 eV). However, the lack of similarity with the structures that appear in the results of the molecular model suggest that the observed structures might also be partially attributed to counting fluctuations. The molecular model results appear more qualitatively similar to the experimental spectrum,

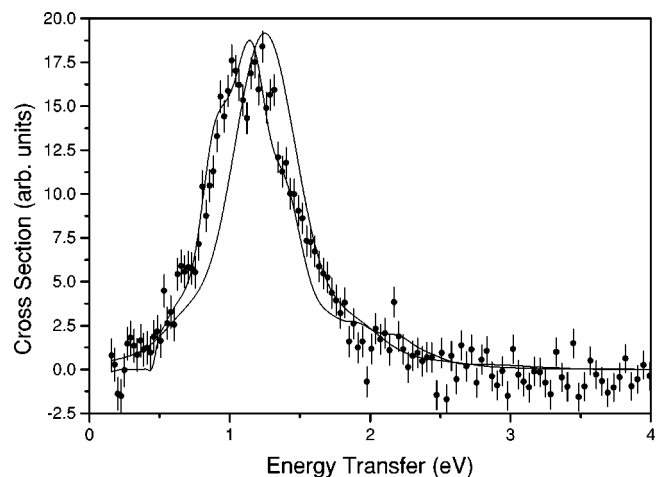


FIG. 3. DINS cross section of liquid hydrogen. The scattering angle is $\theta = 23.41^\circ$. The dots with error bars are the experimental data [normalized using the B factor defined in Eq. (4)]. The line on the left represents the results of the molecular (MYK) model. That on the right is obtained from the atomic (AFP) model.

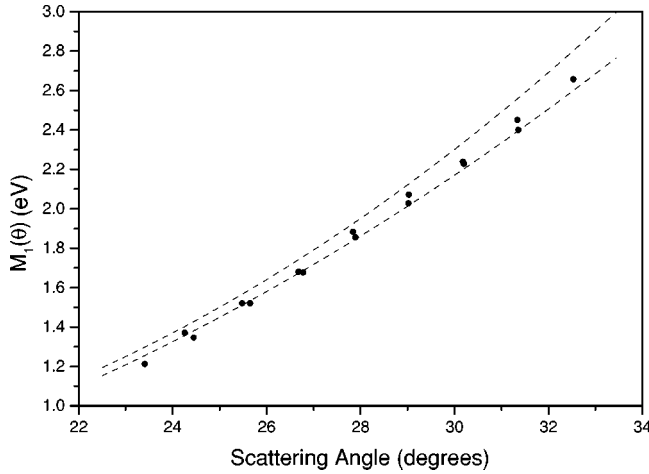


FIG. 4. First moments of DINS spectra as a function of the scattering angle. The upper dashed line represents the atomic model (AFP) while the lower dashed line represents the molecular model (MYK). The black dots are the experimental data evaluated according to Eq. (2).

even though some differences emerge in the high-energy region. This portion of the spectrum, however, is better represented by the atomic model.

IV. DISCUSSION

The overall picture which was described by Figs. 2 and 3 apply equally well to all the sixteen spectra that were taken in this experiment, i.e., in the interval of scattering angles going from 23.4° to 32.5° . From the experimental spectra, given the neutron final energy E_1 and the scattering angle, we could derive the momentum transfer distribution and therefore we could evaluate an average momentum transfer $\bar{q}(\theta)$. The range of \bar{q} is not much different from the values reported in Table I even if the actual values, ranging between 24.4 and 35.6 \AA^{-1} , are a little lower than the atomic model calculation. Therefore, in the whole range of \bar{q} that was tested by the present experiment, neither one of the two models is able to give a satisfactory description of the experiment. A first attempt to discriminate between the two models was carried out computing the first spectral moment of the energy distribution. This is defined by

$$M_1(\theta) = \frac{\int_{-\infty}^{+\infty} d\omega \hbar \omega S(\theta, \omega)}{\int_{-\infty}^{+\infty} d\omega S(\theta, \omega)} \quad (2)$$

and is a function of the scattering angle. The spectral functions $S(\theta, \omega)$ were obtained by multiplying the cross section data by the ratio k_0/k_1 according to the equation

$$\left(\frac{d^2\sigma}{d\Omega dE} \right)_\theta = \left(\frac{k_1}{k_0} \right) |b|^2 S(\theta, \omega). \quad (3)$$

The effective scattering length b is not specified, as it cancels out in Eq. (2).

In Fig. 4 we report the behavior of the first spectral moment as a function of the scattering angle. The upper dashed

line represents the atomic model while the lower dashed line represents the molecular model. The experimental points (black dots) are generally intermediate between the two theoretical lines and tend to lay closer to the molecular model, especially for the low scattering angles. This should be expected, as a low scattering angle corresponds to a low momentum transfer. However, the size of the experimental errors, that could be inferred observing the different values obtained from the left and right detector banks, does not allow a real discrimination between the two models. An even more interesting graph would have been to draw the average energy transfer \bar{E} as a function of $(\hbar q)^2/2$. The slope of this graph should evolve as $1/m$, where m is the effective mass of the recoiling particle, and one should be able to observe the evolution from the molecular to the atomic regime as a function of q . However, this procedure is *only* correct if the energy average is taken by integrating the distribution at constant q . Unfortunately, the present data do not map a sufficiently wide area of the $\{q, E\}$ space to allow a reliable determination of the constant- q spectra. In addition, the differences observed in Fig. 4, do not reflect the real situation that was better depicted by the spectral information (cf. Figs. 2 and 3).

We have no suggestion for a new intermediate model, independent of either the molecular (MYK) or the atomic (AFP) model. However, we have found that a convenient way of describing the present data is obtained using a linear superposition of these two models. In fact, the observed feature that the width of the experimental spectrum is larger than either theoretical result would suggest a mixing of the two models. In addition, one would expect that by increasing the scattering angle, and consequently the average value of the momentum-energy transfer, the experimental data should resemble more and more the atomic model, while the molecular model should become progressively less accurate. Therefore, one should be able to reveal a crossover between the two different regimes by looking at the evolution of the relative weights as a function of the average energy transfer. This is exactly what we have found.

The data were fitted using a linear superposition of the two models according to

$$\frac{d^2\sigma}{d\Omega dE} = B \left[A \left(\frac{d^2\sigma}{d\Omega dE} \right)_{\text{MYK}} + (1-A) \left(\frac{d^2\sigma}{d\Omega dE} \right)_{\text{AFP}} \right]. \quad (4)$$

The amplitude parameter B in Eq. (4) has been introduced to account for the different intensity calibration of the 16 independent detectors. In Fig. 5 we report one of the experimental cross sections ($\theta = 31.36^\circ$) and the best fit obtained using Eq. (4). The agreement is now excellent, as it is testified by the value of the reduced chi-square $\chi_{\text{red}}^2 = 1.276$. Graphs of similar quality were found for all the measured spectra. As a further example, we report in Fig. 6 the spectrum at the lowest scattering angle ($\theta = 23.41^\circ$). Here, the agreement is less spectacular (the value of the reduced chi-square is $\chi_{\text{red}}^2 = 1.608$) but the data are much better represented than by the two models separately (cf. Fig. 3). It is important to stress, once more, that A is the *only relevant fitting parameter*, as B takes only into account the different intensity calibration of the various detectors.

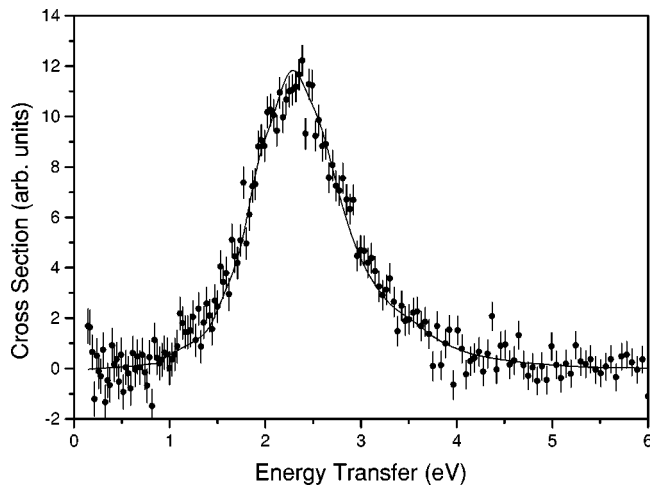


FIG. 5. DINS cross section of liquid hydrogen. The scattering angle is $\theta=31.36^\circ$. The dots with error bars are the experimental data [normalized using the B factor defined in Eq. (4)]. The line represents the best fit using a linear superposition of the molecular (MYK) model and the atomic (AFP) model. The reduced χ^2 of the fit is 1.276.

It is interesting to observe the evolution of the weights A , defined in Eq. (4) as a function of the average momentum-energy transfer or, equivalently, of the scattering angle. What we observe is that, by increasing the scattering angle, the weight of the molecular model (MYK) decreases, and therefore that of the atomic model (AFP) progressively increases. A more effective way of looking at the evolution of the weights A is as a function of the average energy transfer that is defined by Eq. (2). In Fig. 7 we report the values of the weight A , defined in Eq. (4), as a function of the measured energy spectral moment $M_1(\theta)$. The progressive decrease of the importance of the MYK model is apparent and, more interesting, the behavior points to a vanishing of the weight of the molecular model for a sufficiently high energy. Even if the data are not extremely good, we have fitted a straight line

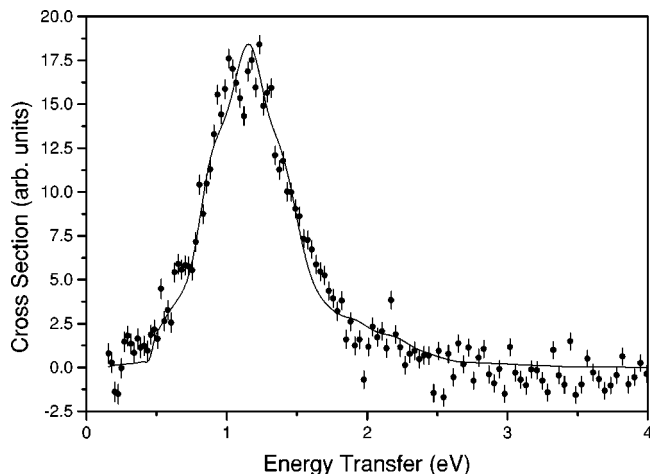


FIG. 6. DINS cross section of liquid hydrogen. The scattering angle is $\theta=23.41^\circ$. The dots with error bars are the experimental data [normalized using the B factor defined in Eq. (4)]. The line represents the best fit using a linear superposition of the molecular (MYK) model and the atomic (AFP) model. The reduced χ^2 of the fit is 1.608.

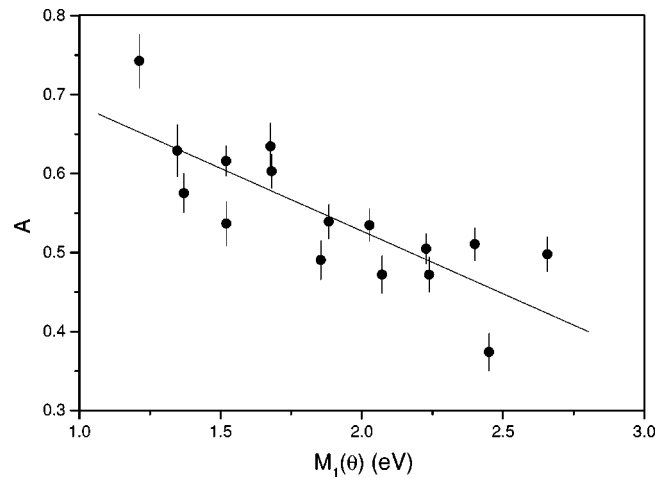


FIG. 7. Relative weights A of the molecular (MYK) model as a function of the measured first spectral moment [cf. Eq. (2)]. The scattering angles are a monotonic function of $M_1(\theta)$. The line is the best linear fit to the points. Its extrapolation gives $A=0$ when $M_1(\theta)=5.5$ eV. The dissociation energy of hydrogen is 4.75 eV.

to the points of Fig. 7. It turns out that $A=0$ for $M_1(\theta)=5.5$ eV, i.e., a value quite similar to the dissociation energy of hydrogen ($E_d=4.75$ eV).

V. CONCLUSIONS

We have carried out a DINS experiment on liquid *para*-hydrogen, in a region of momentum and energy transfer where we expect the emergence of the molecular features of the sample. We have compared the experimental data with the results of two theoretical models: one based on a molecular description of the sample, the second assuming an atomic model. In the calculations, the only inputs were the molecular properties of hydrogen and the effective temperature obtained from the value of the translational kinetic energy of liquid hydrogen derived by our PIMC simulations. No fitting parameters were introduced. Neither one of the two models was able to describe properly the experimental spectra in the explored range of energy transfer. In all cases, we find that the rising part of the experimental spectra (lower energy) was following more closely to the molecular model data, while the high-energy decay was more close to the atomic model. However, the experimental peak of the recoil spectrum was always intermediate between the theoretical calculations involving the two models and its width larger. This suggests an interpretation of the experimental data as a superposition of two mechanisms. In the molecular model, the intramolecular structure is not affected by the collision with the neutron and the molecule reacts as a whole to the scattering event. In the atomic model, instead, the final state of the target nucleus is described by a plane wave. Even if this fact does not imply that the hydrogen molecule is dissociated by the collision of either atom with the neutron, the molecular identity becomes, in this case, conceptually less relevant. At any rate, neither one of the two models is able to reproduce the observed spectra to a quantitative level. It is only when allowing a linear superposition of the two models that the agreement between theory and experiment greatly improves.

The relative weights of the molecular and the atomic model change by changing the scattering angle, and therefore by changing the average energy transfer. The molecular model seems to be more descriptive of the experimental data in the lower-energy region and appears to deteriorate as the average value of the energy transfer approaches the dissociation energy of 4.75 eV. It is worthwhile to note that the atomic model extends its influence down to a rather low energy and seems to contribute to $\sim 30\%$ of the cross section, even for an average energy transfer of 1 eV (cf. Fig. 7). This is a rather surprising result, because this is a relatively

low value with respect to the dissociation threshold of 4.75 eV. However, it appears that the plane wave approximation of the final wave function of the target nucleus is descriptive of a rather large portion of the dynamics of DINS on molecular hydrogen in a relatively low-energy-momentum regime.

ACKNOWLEDGMENT

The technical assistance of the ISIS Instrument Division of RAL is gratefully acknowledged.

-
- ¹V. F. Sears, Phys. Rev. A **5**, 452 (1972).
²V. F. Sears, Phys. Rev. A **7**, 340 (1973).
³V. F. Sears, Phys. Rev. B **30**, 44 (1984).
⁴R. O. Simmons and P. E. Sokol, Physica B **136**, 156 (1986).
⁵R. O. Hilleke, P. Chaddah, R. O. Simmons, D. L. Price, and S. K. Sinha, Phys. Rev. Lett. **52**, 847 (1984).
⁶K. W. Herwig, P. E. Sokol, T. R. Sosnick, W. M. Snow, and R. C. Blasdel, Phys. Rev. B **41**, 103 (1990).
⁷U. Bafile, M. Zoppi, F. Barocchi, R. Magli, and J. Mayers, Phys. Rev. B **54**, 11 969 (1996).
⁸M. Celli, M. Zoppi, and J. Mayers, Phys. Rev. B **58**, 242 (1998).
⁹M. Zoppi, Physica B **183**, 235 (1993).
¹⁰W. Langel, D. L. Price, R. O. Simmons, and P. E. Sokol, Phys. Rev. B **38**, 11 275 (1988).
¹¹K. W. Herwig, J. L. Gavilano, M. C. Schmidt, and R. O. Simmons, Phys. Rev. B **41**, 96 (1990).
¹²J. Mayers, Phys. Rev. Lett. **71**, 1553 (1993).
¹³C. Andreani, A. Filabozzi, and E. Pace, Phys. Rev. B **51**, 8854 (1995).
¹⁴U. Bafile, M. Zoppi, M. Celli, R. Magli, A. C. Evans, and J. Mayers, Physica B **217**, 50 (1996).
¹⁵C. Andreani, D. Colognesi, A. Filabozzi, E. Pace, and M. Zoppi (unpublished).
¹⁶A. C. Evans, J. Mayers, D. N. Timms, and M. J. Cooper, Z. Naturforsch. Teil A **48A**, 425 (1993).
¹⁷D. N. Timms, A. C. Evans, M. Boninsegni, D. M. Ceperley, J. Mayers, and R. O. Simmons, J. Phys.: Condens. Matter **8**, 6665 (1996).
¹⁸I. S. Silvera, Rev. Mod. Phys. **52**, 393 (1980).
¹⁹F. Barocchi, M. Moraldi, M. Santoro, L. Ulivi, and M. Zoppi, Phys. Rev. B **55**, 1 (1997).
²⁰H. M. Roder, G. E. Childs, R. D. McCarty, and P. E. Angerhofer, NBS Tech. Note **641** (1973).
²¹U. Bafile, M. Celli, and M. Zoppi, Physica B **226**, 304 (1996).
²²J. Mayers, Phys. Rev. B **41**, 41 (1990).
²³J. A. Young and J. U. Koppel, Phys. Rev. A **135**, 603 (1964).
²⁴J. Van Kranendonk, *Solid Hydrogen* (Plenum, New York, 1983).
²⁵M. Zoppi and M. Neumann, Phys. Rev. B **43**, 10 242 (1991).
²⁶M. Zoppi and M. Neumann, Physica B **180 & 181**, 825 (1992).